J. Plasma Fusion Res. SERIES, Vol.7 (2006) 68-72

The Stark Effect and Field Ionization in Triplet Rydberg States of Helium Atoms

TAKAHASHI Risako, YAMAKITA Yoshihiro*, HORI Nobutaka, OHNO Koichi

Department of Chemistry, Graduate School of Science, Tohoku University,

Sendai 980-8578, Japan

(Received: 5 October 2004 / Accepted: 9 February 2006)

Abstract

The DC Stark effect is studied for high Rydberg states (principal quantum number $n \geq 15$) of helium atoms in the triplet spin state. A signal is detected through pulsed field ionization by an electric field $F = 6000$ V/cm with a slew rate of 4.0×10^{10} Vcm^{-1}s^{-1}. Stark manifolds are clearly observed in the region below the classical saddle point energy of the Stark field and above the adiabatic pulsed field ionization limit. A detailed Stark map is calculated for magnetic quantum numbers $m = 0$ and $|m| = 1$ states based on matrix diagonalization to explain pulsed-field ionization dynamics. Ionization of the Stark states is well explained by the adiabatic ionization passages.

Keywords:

Stark effect, Rydberg state, metastable helium, field ionization, avoided crossing

1. Introduction

The Stark effect can be utilized for controlling the translational motion of gas-phase atoms [1] and molecules [2] based on a similar principle to that of the Stern-Gerlach experiment. In particular, an electric field gradient opposing the molecular translation can take away translational energy from the molecule when it is switched off abruptly. Indeed Meijer and coworkers have demonstrated deceleration and trapping (25 mK) of neutral ND_3 molecules using fast-switched multi-stage electric fields [2]. Electric-field deceleration is therefore possible for neutral atoms and *non-polar* molecules in Rydberg states, since high Rydberg states gives rise to large Stark shifts in energy. Actually molecular control of deflection and deceleration has been demonstrated for a supersonic beam of non-polar, non-magnetic neutral H_2 [3].

This paper summarizes spectroscopic measurements on the He atom with $n \geq 15$ and $|m| = 0, 1$, and describes the behavior of these states in static and pulsed electric fields. The Stark effect in He has been extensively studied for more than 50 years, and basically established by numerous early studies [4-6], and also by recent studies based on scaled-energy spectroscopy [7,8]. However, to our best knowledge, the reported experimental data are limited to either a narrow range of large n values ($n \approx 40$) [5,6], or different experimental conditions in terms of, e.g., field strength and tunablity of lasers [4]. Hence experimental data are desired for appropriate ranges of n and F, in the unscaled axes of energy and field, and simple theoretical calculations are of practical use rather than sophisticated theoretical treatments, such as WKB-quantum defect theory [4,6]. In this paper, we investigate an experimental "Stark map" for a range of ca. $15 \leq n \leq 20$, and discuss temporal behavior in time-dependent fields using matrix diagonalization of effective Hamiltonian [5,9].

2. Experiment

A schematic overview for the experimental apparatus is shown in Fig. 1. A metastable helium atom beam is produced by a continuous discharge source [10]. A set of three parallel fine grids is placed in the excitation

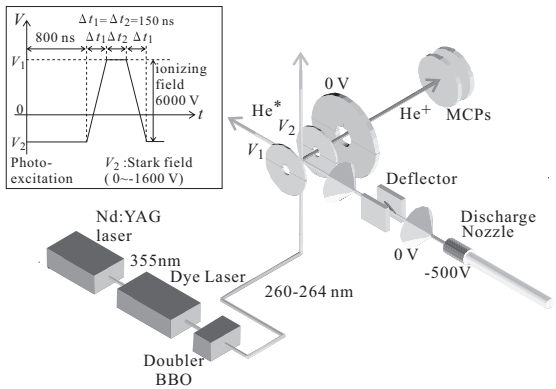

Fig. 1 Experimental apparatus. A shape of ionizing pulsed field is presented in the inset.

Corresponding author's e-mail: yy@qpcrkk.chem.tohoku.ac.jp

region with separation of 1.0 and 1.5 cm respectively. Grid 2 applies a homogeneous DC Stark field of 0 to –1600 V/cm (inset, Fig. 1). The metastable atoms are photo-excited to high Rydberg states by a UV pulsed laser in the presence of the Stark field. Grid 1 generates an ionizing pulsed field of magnitude 6000 V/cm with respect to the Stark voltage, which is controlled by a fast high-voltage pulse generator (DEI PVX-4130). It increases from 0 to 6000 V/cm in 150 ns with a delay time of 800 ns, keeps a constant voltage for 150 ns, and decreases in 150 ns. Spectra are recorded by monitoring the ions as a function of laser frequency.

A UV beam ($\lambda = 259 - 264$ nm, 10 Hz, 6 ns) is provided by a frequency-doubled dye laser pumped by a Nd:YAG laser. The frequency is resonant with one-photon transitions from the intermediate 2^3S state (159856.07760 cm^{-1} above the ground state [11]) to the Rydberg series converging on the ionization threshold ($IE = 198310.7723\,cm^{-1}$). The wavelength of the UV light is calibrated with an iodine cell. The polarization of the laser can be set either parallel or perpendicular to the Stark field, which defines the space quantization axis z. From the intermediate 2^3S state, the Rydberg states with $m = 0$ or $|m| = 1$ are accessible by the parallel or perpendicular polarizations respectively.

3. Calculation

We employ a matrix diagonalization treatment which is essentially the same as those for alkali metals [9] except that the formalism of Edmonds et al. [12] is used to evaluate the radial integral in Eq. (2). The Hamiltonian is of the form

$$H = H_0 + eFz, \tag{1}$$

where the matrix elements of z are given as

$$\langle vlm|z|v'l'm'\rangle = \delta_{m,m'}\delta_{l,l\pm1}\langle vl|r|v'l'\rangle \times \langle lm|\cos\theta|l'm'\rangle, \tag{2}$$

where effective quantum number $v = n - \mu_l$. The diagonal matrix elements of the zero-field Hamiltonian are given by

$$\langle vlm|H_0|vlm\rangle = IE - \frac{R_{\rm He}}{(n-\mu_l)^2}, \tag{3}$$

where $R_{\rm He}$ is the Rydberg constant for the helium atom. The values for the quantum defects μ_l are available in Ref. [11].

4. Results and discussion

4.1 Zero-field spectroscopy

Figure 2 shows the zero-field spectrum of the 1snp^3P Rydberg series of He; the levels resolved are in the range $n = 15 - 58$ and a single quantum defect [11] reproduces the experimental values with an accuracy 0.075 cm^{-1}. The intensity distribution in the region of $n \geq 18$ reflects the ionization rate and oscillator strength. All the transitions are recorded through pulsed-field ionization in a total duration 450 ns (see inset, Fig. 1) with a delay time of 800 ns. The Rydberg states with larger n can be field ionized for a longer interval due to the rise time of the field. Moreover the ionization rate dramatically decreases as n decreases in an electric field. The oscillator strength for the ns-n'p transition decreases as n'p energy increases since the nodes of the bound np wavefunction become close together with increasing energy [6,13]. In the region below $n = 18$ the intensity decreases towards zero as it goes to $n = 15$. This is likely due to the slow ionization rates in a short time window of the ionizing pulse for the lower-n Rydberg states.

4.2 Stark spectroscopy and field ionization dynamics

Figure 3 (b) presents the Stark spectra of the $m = 0$, 1 snp^3P Rydberg states recorded in homogeneous electric fields of 0 – 1000 V/cm. At field larger than 400 V/cm, additional peaks are observed in the low-wavenumber sides of the Stark manifolds. These peaks originate from $l = 0$ states and gain their intensities by mixing with $l = 1$ states. The magnitude of mixing can be recognized as the increase of their intensities relative to the Stark manifolds. The mixing of different l-states can be viewed more quantitatively in Stark maps (Fig. 3 (a)). Separation width at avoided crossings of the upper and lower states differs significantly between the cases of $m = 0$ and $|m| = 1$ (Fig. 4 (a)), which is commonly found in alkali-metal atoms [9]. The width which is approximately twice the magnitude of the off-diagonal matrix elements $\langle nlm|z|n'l'm'\rangle$ in Eq. (2) is larger in the $m = 0$ states, where the lobe of the electronic wavefunction of a Rydberg electron extends to the same z-direction, than in the $m \neq 0$ states in which there are degenerate wavefunctions pointing to various directions. The width is estimated to be 1 cm^{-1} and 0.3 cm^{-1} at the first avoided crossing between $n = 15$ and 16 extreme states.

Field ionization takes place from the position of the applied Stark field towards the right-hand side of the figures, where Stark states couple to the continuum. It is commonly known that a Stark sub-level populated traverses adiabatically or diabatically depending on the slew rate of the ionizing pulsed field [14]. The mechanism determines the threshold for field ionization. If field ionization is adiabatic, it goes along zig-zag passages and the threshold would be approximately

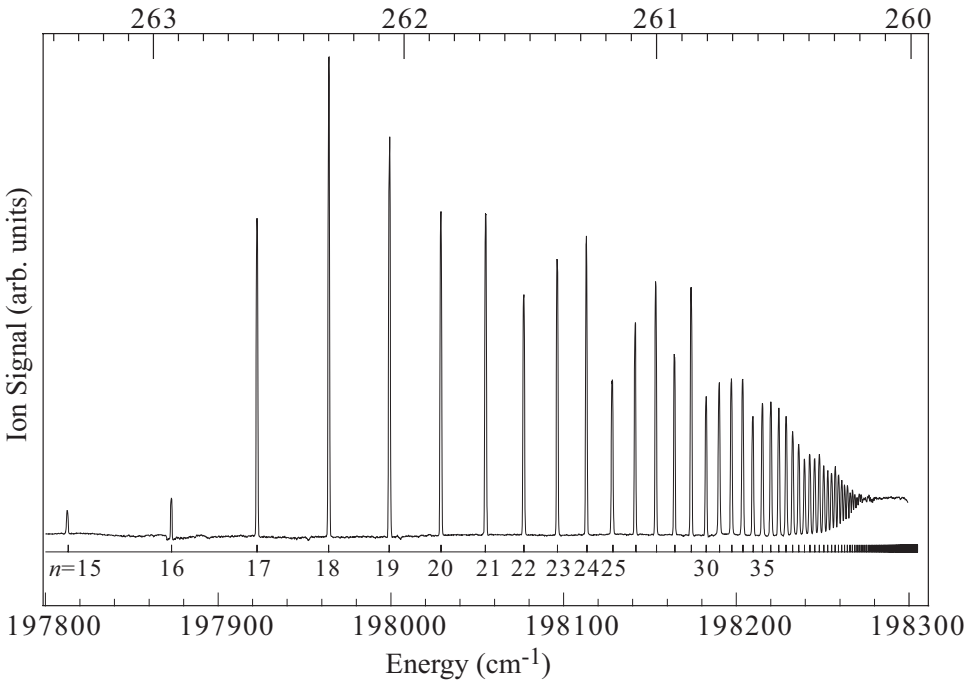

Fig. 2 Zero-field spectrum of the $1snp\,^3P$, $|m|=1$ Rydberg series of He.

at the classical saddle point energy, 6.12 $\sqrt{F}(\mathrm{cm}^{-1})$ below the ionization energy, where F is given in V/cm (Figs. 3 (a) and 4 (a)). Probability of the diabatic transition calculated for the slew rate of the ionizing pulse $S = \mathrm{d}F/\mathrm{d}t = 4.0\times10^{10}\,\mathrm{Vcm}^{-1}\mathrm{s}^{-1}$ is $P_\mathrm{D} = 1.9\times10^{-13}$ in the $|m| = 1$ case, assuming energy change for the above mentioned two states is linear. Therefore diabatic ionization is highly unlikely, and the Rydberg states of both $m = 0$ and $|m| = 1$ overwhelmingly ionize through the adiabatic passages.

Comparisons between experimental and calculated spectra are given in Figs. 3 and 4 for the $m = 0$ and $|m| = 1$ states, respectively. First the experimental intensity distributions of the Stark manifolds are in reasonable agreements with the calculated ones, of which intensities are borrowed from the optically-allowed np states. It follows that the transition intensities reflect predominantly the magnitude of mixing with the np states. The Stark manifolds show asymmetric distributions until they become nearly complete hydrogenic manifolds.

Second it is remarkable that the observed number of sub-levels in the $n = 16$ Stark manifolds is fewer than the calculated ones (low-energy sides in Fig. 4 (c)). This is likely to be connected with the ionization threshold, which is determined by the relation between the adiabatic ionization passage and the classical saddle-point energy. In Figs. 3 (a) and 4 (a) the lowest Stark sub-levels which can be field ionized are shown as bold lines. In the case of $m = 0$, the lowest sub-level in the $n = 16$ manifold which is associated with 16s state meets the saddle point energy at 6000 V/cm. On the contrary, the lowest sub-level of the $n = 16$, $|m| = 1$ manifold is located far below the energy. The saddle point energy for the $m \neq 0$ states is also lifted by a few % from those for $m = 0$ states, owing to the centrifugal barrier of a Rydberg electron [13]. Hence the solid zigzag line depicted in Fig. 4 (a) marks the lowest states which can ionize by the field, and precisely corresponds to the observed threshold for ionization.

4.3 Ionization rate and tunnelling ionization

The ionizing field employed in the present measurements holds its peak for 150 ns, therefore the ionization rate is required to exceed $\Gamma = 4.7\times10^6\,\mathrm{s}^{-1}$ for the states to be detected. On the other hand, the ionization rate for the H atom shows that the rate for the highest extreme sub-levels is much smaller than those for the lowest states [15]. However, in the non-hydrogenic atom, Stark states can mix with each other, and the amount of mixing with the fast-ionizing sub-level would effectively determine the ionization rate. Observation of the $n = 15$ Rydberg state (Fig. 2) is likely to be connected with tunnelling ionization, since it lies below the ionization threshold.

5. Conclusions

The experimental spectra are fairly well explained by a simple calculation based on matrix diagonalization of the effective Hamiltonian. Possibility for the diabatic ionization at the avoided crossings is negligibly small for a field of a slew rate $S = 4.0\times10^{10}\,\mathrm{Vcm}^{-1}\mathrm{s}^{-1}$. A

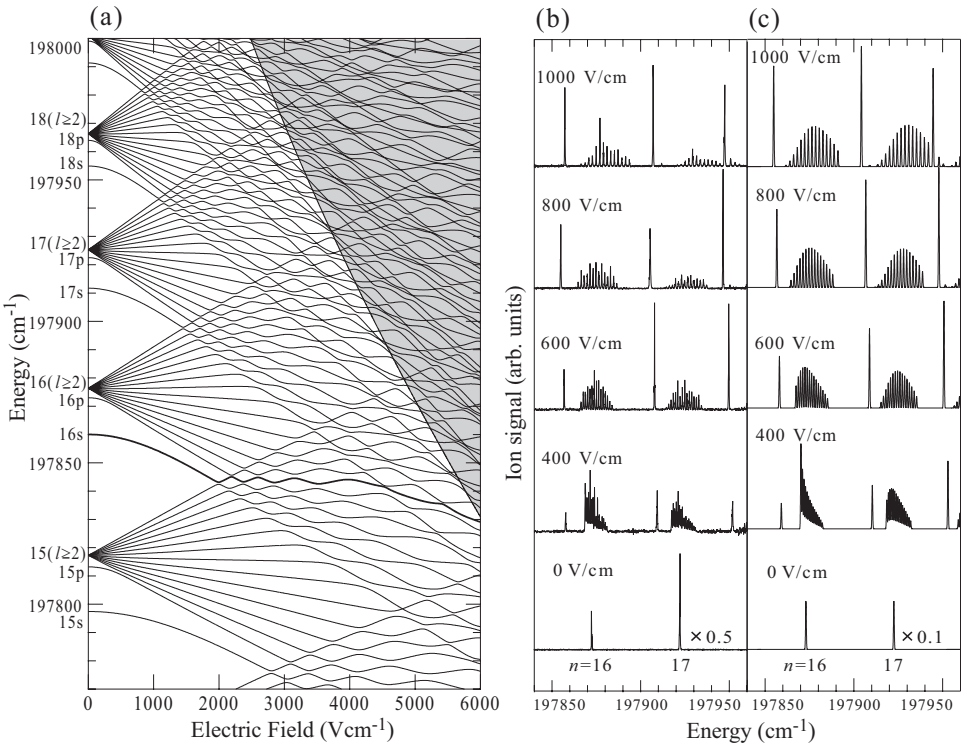

Fig. 3 (a) Stark map for $m = 0$ Rydberg states. Comparison between (b) experimental and (c) calculated spectra of $n = 16$ and 17 Stark manifolds. The simulation has been convoluted with a Gaussian bandwidth (FWHM) of 0.5 cm^{-1}. The grey region represents the continuum beyond the classical saddle point energy.

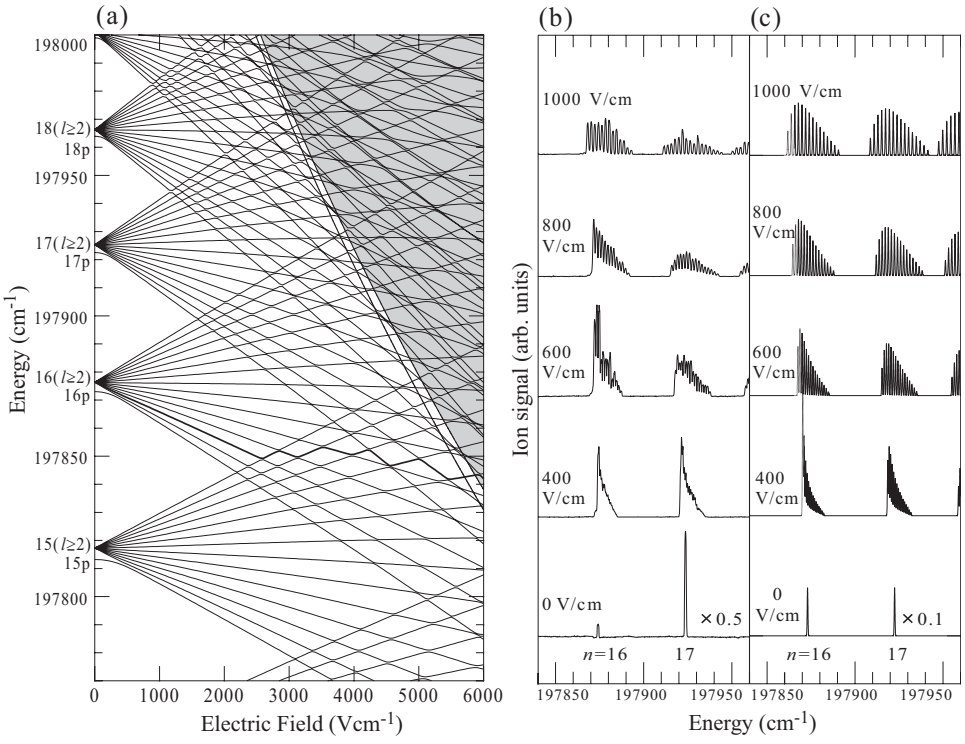

Fig. 4 (a) Stark map for $|m| = 1$ Rydberg states. (b) Experimental and (c) calculated spectra. See also the caption to Fig. 3.

pulsed electric field of a height 6000 V/cm ionizes Rydberg states adiabatically, whereas state $n = 15$ is most likely to ionize through tunnelling ionization. Some of the Stark sub-levels of the $n = 16$ manifold are not observed in the $|m| = 1$ case. These sub-levels are cut-off by the ionization threshold, which corresponds to the increased height of the classical saddle point energy due to the centrifugal barrier. The high Rydberg states studied here are triplet states and radiatively decay to the metastable 2^3S state of which lifetime is 4200 s.

Therefore if decelerating and trapping triplet Rydberg He atoms is possible, it could lead to new experimental techniques for future studies involving a translationally cold bunch of the metastable He (2^3S).

Acknowledgements

This work was financially supported by the MEXT through a Grant-in-Aids for Young Scientists (A) (No 14703003), and by the Matsuo Foundation through a research grant. The authors thank Professor T. P. Softley for encouraging discussions.

References

[1] T. Breeden and H. Metcalf, Phys. Rev. Lett. **47**, 1726 (1981).

[2] H.L. Bethlem and G. Meijer, Int. Rev. Phys. Chem. **22**, 73 (2003).

[3] Y. Yamakita, S.R. Procter, A.L. Goodgame, T.P. Softley and F. Merkt, J. Chem. Phys. **121**, 1419 (2004) and references therein.

[4] W. van der Water, D.R. Mariani and P.M. Koch, Phys. Rev. A **30**, 2399 (1984).

[5] C.T.W. Lahaye and W. Hogervorst, Phys. Rev. A **39**, 5658 (1989).

[6] A. Nussenzweig, E.E. Eyler, T. Bergeman and E. Pollack, Phys. Rev. A **41**, 4944 (1990).

[7] R.V. Jensen, H. Flores-Rueda, J.D. Wright, M.L. Keeler and T.J. Morgan, Phys. Rev. A **62**, 053410 (2000) and references therein.

[8] C.T.W. Lahaye and W. Hogervorst, Phys. Rev. A **58**, 3043 (1998).

[9] M.L. Zimmerman, M.G. Littman, M.M. Kash and D. Kleppner, Phys. Rev. A **20**, 2251 (1979).

[10] K. Ohno, T. Takami, K. Mitsuke and T. Ishida, J. Chem. Phys. **94**, 2675 (1991).

[11] W.C. Martin, Phys. Rev. A **36**, 3575 (1987).

[12] A.R. Edmonds, R. Pullen, J. Picart and N. Tran Minh, J. Phys. B **12**, 2781 (1979).

[13] T.F. Gallagher, *Rydberg Atoms* (Cambridge University Press, Cambridge, 1994).

[14] J.R. Rubbmark, M.M. Kash, M.G. Littman and D. Kleppner, Phys. Rev. A **23**, 3107 (1981) and references therein.

[15] R.J. Damburg and V.V. Kolosov, J. Phys. B **12**, 2637 (1979).